

Fractional charges in emergent neutral modes at the integer quantum Hall effect

Hiroyuki Inoue¹, Anna Grivnin¹, Nissim Ofek², Izhar Neder³, Moty Heiblum¹, Vladimir Umansky¹ and Diana Mahalu¹

¹Braun Center for Submicron Research, Department of Condensed Matter Physics,
Weizmann Institute of Science, Rehovot, Israel

²Departments of Physics and Applied Physics, Yale University, New Haven, CT, USA

³Raymond and Beverly Sackler School of Physics and Astronomy, Tel-Aviv University, Tel
Aviv, 69978, Israel

Charge fractionalization is a possible emergent excitation in a low-dimensional system of interacting electrons. A known example is that of fractional charges in the fractional quantum Hall effect (FQHE) regime, which is a consequence of strong Coulomb interaction among the electrons whose kinetic energy is quenched by the strong magnetic field. Alternatively, the integer QHE (IQHE), with electrons behaving largely as *independent particles* in Landau levels (LLs), lacks such fractionalization. However, for integer LLs filling $v=2, 3, \dots$, electrons propagate in copropagating adjacent chiral edge channels, and thus interact and modify the non-interacting LLs. For example, at $v=2$, an electron injected selectively into a single non-interacting (bare) edge channel is expected to decompose into a ‘fast’ mode and a ‘slow’ mode in the region of interaction; each mode carry fractional charges shared between the two bare channels. Here, we report our sensitive shot noise measurement that affirms the presence of such fractionalization in $v=2$. Injecting partitioned current into a ‘hot’ edge channel led to low frequency shot noise in the adjacent currentless ‘cold’ edge channel after it had been partitioned. Controlling the partitioning of the hot and cold channels allowed a determination of the fractional charges in both channels as well as the channels’ velocity difference. This approach can be extended to study interaction in two-dimensional systems with a topology dictating edge channels transport.

Charge fractionalization is an exotic manifestation of low dimensional correlated electrons. Fractionally charged quasiparticles in the FQHE¹⁻⁶ and in quantum wires⁷ provide examples. Here, we employ a high mobility two dimensional electron gas in the IQHE regime and at filling factor $\nu=2$ (spin split lowest LL). At low-energies the transport takes place solely at the sample's periphery via gapless chiral (downstream) edge channels, with channel conductance $G_0=e^2/h$, where e the electron charge and h the Planck constant⁸⁻⁹. Due to the spatial separation between the channels, each channel can be manipulated (reflected, transmitted, or redirected) individually; customarily with a quantum point contact (QPCs) constriction. A recently discovered upstream neutral edge modes in hole-conjugate FQHE states, resulting from edge reconstruction¹⁰⁻¹², revealed the importance of inter-channel Coulomb interaction (in this case it was also accompanied by inter channel tunneling). Evidently, Coulomb interaction takes place also in the IQHE regime; as had been already reported and analyzed in studies that observed 'lobe structures' in the visibility of interferometers¹³⁻¹⁴; interaction mediated dephasing¹⁵⁻¹⁸; and energy equilibration among edge channels¹⁹⁻²³. Moreover, inter-channel interaction between copropagating channels had been already predicted to give rise to downstream charge density modes propagating at different velocities and carry fractional excitations²⁴⁻²⁹. While the existence of modes with different dispersion relations had been already reported³⁰, the charge of their excitations has not been determined yet. Here, we demonstrate an observation of fractionally charged excitations in the IQHE, with two interacting chiral edge channels, via low frequency shot noise measurements^{3,31-33}.

Employing a channel selective quantum point contact (QPC) allows injecting partitioned electrons in one of the two copropagating channels (a 'hot' channel). Inter-channel interaction (without tunneling) will induce local charge imbalance in the 'cold' channel, which upon partitioning by another QPC, will bare a finite currentless shot noise (fluctuations around zero net current). Measuring the dependence of that noise on the partitioned 'hot' current, allowed the determination the interaction strength and the excitations charge.

Before delving into the details of our experiment, it might be illuminating to present an intuitive model of the system. The resulting excitations in the two channels (1 & 2) can be regarded as

fractionally charged dipoles flowing downstream, with the spin degree of freedom play no role here. Assume short range inter-channel interaction $uh\delta(x_1-x_2)$, the energy density of the interacting channels $\varepsilon = h(v_1\rho_1^2 + v_2\rho_2^2 + u\rho_1\rho_2)$, with $\rho_1(x_1)$ and $\rho_2(x_2)$ being the number densities and v_1 and v_2 the velocities of the non-interacting channels. As shown in Fig. 1a, injecting an electron in channel 1 (via a partitioning QPC1 with probability T_1), gives birth to two modes distributed between channels 1 and 2: (i) a ‘slow’ mode, consisting of a particle-like charged $+(1-\alpha)e$ and a hole-like charged $-\beta e$, in channel 1 & 2, respectively; (ii) a ‘fast’ mode, consisting of particles-like charged $+\alpha e$ and $+\beta e$, in channel 1 & 2, respectively. Here, $\alpha=(1+\cos\theta)/2$, $\beta=0.5\sin\theta$, and $\tan\theta=u/\Delta v$ ($0<\theta<\pi/2$) with $\Delta v=v_1-v_2$. The two modes propagate at velocities $v_{\pm}=\bar{v}\pm\frac{1}{2}\sqrt{(\Delta v)^2+u^2}$, where $\bar{v}=(v_1+v_2)/2$ and + (-) stand for fast (slow). Noting that when the two channels have equal velocities, $\alpha=\beta$, and the ‘slow’ mode is neutral. Moreover, for $v>0$, $4v_1v_2>u^2$ must be satisfied. Measuring the charges of the fractionalized wave packets by fast chopping in order to separate the ‘fast’ mode from the ‘slow’ one, necessitates rather challenging high frequency measurements. Hence, since channel 2 (the ‘cold’ channel) carries always zero net current but a fluctuating ‘neutral excitation’, $+\beta e$ and $-\beta e$, we chose to characterize these fractionally charged quasiparticles via continuous low frequency shot noise measurements, which arise by partitioning stochastically the stream of quasiparticles in channel 2.

Results

Measurement scheme

Our 2DEG was embedded in a ubiquitous GaAs-AlGaAs heterostructure. The resultant patterning is shown in the SEM micrograph in Fig. 1b with a magnified view of the core part below. The light blue region is a mesa where the 2DEG exists; the light gray curves are metallic gate electrodes; yellow pads are ohmic contacts, where S1 & S2 denote source contacts, G grounds, and A1 & A2 amplifier contacts (each loaded with a resonant circuit, $f_0\sim 790\text{kHz}$, followed by a cryogenic amplifier). The two QPC constrictions, separated by an interaction region, $l=8\mu\text{m}$, with its potential being modified by an additional side gate off the mesa, SG, whose voltage was kept at -500mV (gates are green in Figs. 1c & d). In configuration C1 the outer channel plays the role of the ‘hot’ channel (channel 1), while in configuration C2 the inner channel plays that role. In configuration C1 (Fig. 1c), the source current $2I$ (thick red lines) is shared equally between the two

edge channels. Constriction QPC1 fully reflects the inner channel while partitions the outer channel (T_1, R_1 , dotted heavy red line). Two ‘cold’ edge channels, emanating from the G contacts, also impinge at QPC1 (thin blue lines), with the outer is fully transmitted and the inner fully reflected. The reflected ‘cold’ channel (thick blue line) flows in close proximity to the partitioned outer channel, with both reaching QPC2. There, the outer channel is fully transmitted and inner one is being partitioned (T_2, R_2 , dotted thick blue line), with its excess current noise (spectral density, S_i) monitored at A1. We employ configuration C1 (C2, shown in Fig. 1d, with the role of the two channels reversed) to measure the dependence of excess noise of the cold channel on T_1 of the ‘hot’ channel (T_2 of the ‘cold’ channel). Such arrangement is chosen since the transmission probability T_1 of the outer ‘hot’ channel is fairly constant with energy. We stress that suppressing the inter-channel tunneling current (below 5×10^{-4} of source current) was crucial for reliable results.

The measured noise is composed of excess shot noise, thermal (Johnson-Nyquist) noise³¹, and preamplifier current and voltage noises³². The ‘hot’ channel is being partitioned stochastically at QPC1 with transmission probability T_1 , with a resultant ‘white’ excess noise, $S_i = 2eIT_1(1 - T_1)(\coth x - x^{-1})$, where S_i its ‘zero frequency’ spectral density (frequency $\ll eV/h$), with $x = eIG_0^{-1}/2k_B\Theta$, k_B Boltzmann constant³¹⁻³³. The spectral density depends linearly (quadratically) on high (low) I for a given electron temperature, which was found to be $\Theta \sim 20$ mK. The spectral density of the partitioned ‘hot’ channel was measured as function of T_1 . Its normalized magnitude was plotted in the inset of Fig. 2a. The expected dependence $\propto T_1(1 - T_1)$ is observed. Note that, due to the multi-terminal configuration, the amplifier is fed by a constant Hall resistance, and thus the current noise of the preamplifier and the Nyquist noise were both independent of QPC transmission. However, in the present experiment we expect to measure shot noise without net current in the partitioned, unbiased, ‘cold’, channel - a peculiar situation.

The fractionalization noise

The net current and excess noise S_i in A1 were measured in configuration C1 at current $I = -1.6$ to $+0.4$ nA, for different QPC transmissions T_1 (0.06-0.94), while QPC2 was kept at constant transmission $T_2=0.5$ (Fig. 2a). As the injected current (in absolute value) increased, the excess noise S_i increased; however, without net current. The dependence of the excess noise in the partitioned ‘cold’ channel on I resemble roughly a standard excess noise. However, it is interesting

to notice that the low noise rounding (near zero current) is wider than the corresponding one in the hot channel. We return to this point later again. A dependence of the excess noise on T_1 is shown in Fig. 2b (normalized to $T_1 \approx 0.5$); obeying a simple dependence $[T_1(1-T_1)]^{\gamma_1}$, with $\gamma_1=0.70$ (for comparison, curves with $\gamma_1=0.5$ & 1.0 are also plotted).

Similar measurements were repeated with configuration C2, where the role of the two channels was reversed. The dependence of S_i in the outer channel (now the ‘cold’ channel) on the injected current into the inner channel (now the ‘hot’ channel, partitioned with $T_1=0.5$) is plotted in Fig. 3a. Different partitioning T_2 of the ‘cold’ channel (in range 0.1–1) were employed. In the same manner as previously, a dependence $[T_2(1-T_2)]^{\gamma_2}$ of the noise was found (Fig. 3b); with $\gamma_2=0.95$. This time the partitioning appears to be nearly binomial in T_2 .

Since the predicted fractional excitations in the ‘hot’ channel is αe and $(1-\alpha)e$, it is only natural to ask whether those quasiparticles can be measured via shot noise. Partitioning the ‘hot’ channel with QPC2, after it interacted with the ‘cold’ channel, led, however, to the ‘boring’ spectral density of independent partitioned electrons, $S_i=2eIT_1T_2(1-T_1T_2)$, for a wide range of T_1 and T_2 (data not shown); namely, revealing charge e . This result can be understood by realizing that the low frequency shot noise can only reflect tunneling events of electrons in the QPC; being in the IQHE regime, only electrons are allowed to back scatter by the QPC.

Discussion

Comparing with theory

Several recent theories considered our present experimental scheme²⁷⁻²⁹. Particularly, Ref. 29 provided a platform for how to extract the *mixing angle* θ ($\tan \theta=u/\Delta v$) and the fractional charge βe ($\beta=0.5 \sin \theta$) from the measured spectral density S_i of the ‘cold’ channel at zero temperature. This paper provides the missing connection between θ and the strength of the noise (expressed by the Fano factor F (see Fig. 4a)) as well as with the noise dependence on T_1 , namely, γ_1 (see Fig. 4b). Defining the Fano factor $F(\theta)=S_i/S_{Ref}$, which reflects the charge of the partitioned quasiparticles $e^*=Fe$, where the reference spectral density is $S_{Ref}=4eIT_1R_1R_2$, being the excess noise due to stochastically back scattering of a random train of electrons and holes. The prediction

assumes only inter-channel interaction, namely, void of interaction with an external environment and for $R_2=1-T_2<<1$. With $0<\theta<\pi/2$, γ_1 was calculated to span $0.68 \leq \gamma_1(\theta) \leq 1$. As shown in Fig. 4b, for $\theta=\pi/2$ the calculated $\gamma_1=0.68$ - the case when the bare channels' velocities are equal, $\Delta v=0$, and $\beta=\alpha=0.5$ (the 'slow' mode, shared by the two LL's, is *neutral*). Approaching the non-interacting case, $\theta\rightarrow 0$, the 'cold' channel has a diminishing noise, and $\gamma_1\rightarrow 1$. Note also that $\gamma_1=0.5$ (outside the scale in Fig. 4b) stands for the two channels fully thermalizing along the interaction region due to interaction with the environment. Plotting in Fig. 4a the expected fractionalization charge $\beta=(\sin \theta)/2$, which was evaluated with the simple model above, we find a nice agreement with the numerical evaluation of expected fractional charge expressed by $F(\theta)$ ²⁹.

The fractional charge and velocities

Noting that obtaining $\gamma_2=0.95$, with excess noise being nearly binomial in T_2 , namely, linearly dependent on R_2 for $R_2\rightarrow 0$, justifies the perturbative treatment in R_2 in the theory²⁹. Comparing our data with Ref. 29, our determined $\gamma_1=0.70$ falls within the predicted range (void of interaction with the environment), leading to a mixing angle $\theta\sim\pi/3.1$, $u/\Delta v=1.56$, and $F(\pi/3.1)=0.47$ (Fig. 4). This prediction is compared with the measured Fano factor (the slope of the excess noise in the range $-1.2\text{nA} \leq I \leq -0.8\text{nA}$ for $T_1=0.5$ and $T_2=0.1$ divided by $4eT_1R_1T_2R_2$); found remarkably to be $F=0.46$. Verifying consistently the fractional charges are $\beta e=0.42e$ in the 'cold' channel and $\alpha e=0.77e$ in the 'hot' channel.

While most of the parameters of the system had been extracted, the strength of the interaction u is still missing. In a similar configuration (performed by our group in Ref. 15); applying a DC bias of $19\mu\text{V}$ to the inner channel of $v=2$, resulted in 2π phase shift in a coupled interferometer formed by the inner channel being $10\mu\text{m}$ long; suggesting an addition of one electron. Therefore, the mutual capacitance between the channels can be estimated as $C\sim 0.8\text{fF}/\mu\text{m}$. Note that the logarithmic dependent Coulomb interaction distance makes the exact number less important. The conversion relation to $u=e^2/hC$ leads to $u=4.5\times 10^4\text{m/s}$, yielding $\Delta v=2.9\times 10^4\text{m/s}$ (with the minimum average velocity $2.7\times 10^4\text{m/s}$, deduced from $v=0$). The excessive 'rounding' of the excess noise vs. current traces may result from an overlap of the fractional wave packets ($\pm\beta e$) at low I ; thus

suppressing the measured noise in the ‘cold’ channel. However, additional experiments must be performed to verify this effect.

With all this said, it might be useful to provide also an intuitive picture of the mechanism leading to the excess noise in the ‘cold’ channel. Partitioning the DC current in the ‘hot’ channel by QPC1 leads to a wideband current fluctuations with a cutoff at frequency I/e . Obviously, the inter-channel capacitance $Cl=e^2l/hu$ induces high frequency displacement current noise in the ‘cold’ channel, with a low frequency cutoff that depends on the Cl/G_0 time constant (much higher than our measurement frequency). However, stochastic partitioning of the unbiased channel by QPC2 redistributes the high frequency spectrum over the entire spectrum (up to the cutoff frequency) - yet with zero net current.

In summary, observing neutral modes, with zero net current, in an unbiased, interacting, edge state in the IQHE regime (filling factor, $v=2$), allowed a determination of the fractional excitations that form the neutral modes. The neutral modes were characterized by an emerging shot noise after partitioning by a quantum point contact; allowed also the determination of the interaction energy and the relative velocities of the two channels void of interaction. Our scheme opens a way to probe Coulomb correlations in multiple 1D channels of other QHEs and topological insulators.

Methods

Experimental setup

The device was fabricated on a GaAs/AlGaAs heterostructure; with 2DEG embedded 130nm below the surface whose carrier density is $8.2 \times 10^{10} \text{ cm}^{-2}$ and dark mobility is $4.2 \times 10^6 \text{ cm}^2/\text{Vs}$ at 4.2K. The constrictions QPC1 and QPC2, formed by negatively biased split-gates (5nm Ti/15nm Au) with a 600nm wide opening, are separated by center-to-center distance $l=8\mu\text{m}$. Contacts S1, S2, A1, A2, and G, are made of the ubiquitous alloyed AuGeNi. The grounded contacts were tied directly to the cold finger of the dilution refrigerator at 10mK. All the measurements were done at the magnetic field $B=1.7\text{T}$, where the plateau of the bulk filling factor 2 with longitudinal resistance $R_{xx} \sim 0\Omega$ and Hall resistance $R_{xy}=(2G_0)^{-1} \sim 12.9 \text{ k}\Omega$. The noise signal at A1 and A2, filtered with an LC circuit tuned to 790 kHz, was first amplified by a cooled, home-made, preamplifier with voltage gain 11.6, and subsequently by a room temperature amplifier (NF-220F5) with voltage gain 200, followed by a spectrum analyzer with the bandwidth of 10 kHz. The total background noise was $280\text{pV}/\sqrt{\text{Hz}}$ at the resonant frequency. For the transmission measurement, $0.5\mu\text{V}_{\text{RMS}}$ at the resonant frequency, with or without an accompanying DC voltage, was applied at source S1 (S2) and measured at A1 (A2) with the bandwidth of 30Hz. The tunneling current was monitored by increasing the excitation amplitude up to ten times on top on the DC current biases.

Acknowledgements

We thank B. Rosenow, M. Milletari, Y. Oreg, and G. Viola for helpful discussions and H. K. Choi for his technical help. We acknowledge the partial support of the Israeli Science Foundation (ISF), the Minerva foundation, the US-Israel Bi-National Science Foundation (BSF), and the European Research Council under the European Community's Seventh Framework Program (FP7/2007-2013)/ERC, Grant agreement # 227716.

Figures

Figure 1. Schematics of the experiment. **a**, An ordered train of electrons driven from the source (S) transmit the QPC1 with a probability T_1 and decompose into fast and slow modes. The fast mode consists of fractional charges αe (βe) on channel 1 (2) and the slow mode consists of fractional charges $(1-\alpha)e$, $(-\beta e)$ on channel 1 (2). The pairs of $\pm \beta e$ are partitioned at QPC2 with a transmission probability T_2 , generating a low-frequency shot noise to be detected at the amplifier (A). **b**, SEM image of the employed device fabricated on GaAs/AlGaAs. The mesa is blue-highlighted. The yellow pads are ohmic contacts, sources (S1&S2), amplifiers (A1&A2), grounds (G). The gray curves are metallic gates, QPC1, QPC2, and side gate (SG). Below, a magnified view of the core part. The region between the QPCs is the interaction region. **c**, The configuration 1 (C1). S1 and A1 were employed. The red and the blue arrows are the hot and the cold channels. The biased outer channel is the channel 1 here. QPC1 and QPC2 were tuned to transmission probabilities T_1 and T_2 for corresponding channels. For various T_1 transmitting only the biased outer channel, T_2 was set to 0.5 to reflect the unbiased inner channel to A1. **d**, Configuration 2 (C2). S2 and A2 were employed. The biased inner channel is the channel 1 here. T_1 was set to 0.5 and the reflected inner channel was directed to QPC2 with various T_2 to partition the fluctuating but unbiased outer channel.

Figure 2. | Excess noise as a function of T_1 . **a**, The excess noise traces, measured with the configuration C1, as a function of I for several T_1 with fixed $T_2=0.5$ are shown. Noise traces of selected T_1 are shown. In the inset plots, by scaling the trace at $T_1 = 0.5$ to unity, relative noise magnitude of the hot channel at different T_1 behaves as the independent Fermionic one. **b**, Relative magnitude of the excess noise as a function of T_1 , normalized to the one at $T_1=0.5$. The excess noise is proportional to $[T_1(1-T_1)]^{\gamma_1}$, where $\gamma_1=0.70$ for $T_2=0.5$. For comparison, curves with $\gamma_1=0.5$ and 1.0 are also plotted.

Figure 3. | Excess noise as a function of T_2 . **a**, The excess noise traces, measured with the configuration C2, as a function of I for selected T_2 are shown. Similar excess noise was again observed. **b**, Relative magnitude of the excess noise as a function of T_2 , normalized to the one at $T_2=0.5$, is plotted. The excess noise is proportional to $[T_2(1-T_2)]^{\gamma_2}$, where $\gamma_2=0.95$ with $T_1=0.5$.

Figure 4 | Theoretical Fano factor $F(\theta)$ and exponent $\gamma_1(\theta)$ (Ref. 29). Theoretical plots relevant to the present setup and the fractionalization excess noise S_i . The mixing angle θ therein was modified to fit our notations. **a**, The Fano factor $F=S_i/S_{Ref}$ ($S_{Ref}=4eIT_1R_1R_2$) representing the fractional charge in the cold channel ($e^*=Fe$), plotted as function of the mixing angle. The red dots are the theory and the blue curve depicts $\beta=0.5\sin\theta$, based on the simple model in the paper. The latter model and the numerical one²⁹ show a remarkable agreement. **b**, The exponent γ_1 plotted as function of the mixing angle based on the numerical computation²⁹. The experimentally obtained γ_1 yields a mixing angle $\theta\sim\pi/3.1$ ($\tan\theta=u/\Delta v=1.56$), which reads $F=0.47$, $\beta=0.42$ and $\alpha=0.77$.

References

1. Laughlin, R. B. Anomalous quantum Hall effect: An incompressible quantum fluid with fractionally charged excitations. *Phys. Rev. Lett.* **50**, 1395-1398 (1983).
2. Wen, X. G. Chiral Luttinger liquid and the edge excitations in the fractional quantum Hall states. *Phys. Rev. B* **41**, 12838–12844 (1990).
3. de-Picciotto., R. Reznikov, M., Heiblum, M., Umansky, V., Bunin, G. & Mahalu, D. Direct observation of a fractional charge. *Nature* **389**, 162-164 (1997).
4. Saminadayar, L., Glattli, D. C., Jin, Y. & Etienne, B. Observation of the $e/3$ fractionally charged Laughlin quasiparticle. *Phys. Rev. Lett.* **79**, 2526-2529 (1997).
5. Martin, J., Ilani, S., Verdene, B., Smet, J., Umansky, V., Mahalu, D., Schuh, D., Abstreiter, G. & Yacoby, A. Localization of fractionally charged quasi-particles. *Science* **305**, 980-983 (2004).
6. Ofek, N., Bid, A., Heiblum, M., Stern, A., Umansky, V. & Mahalu, D. The role of interactions in an electronic Fabry-Perot interferometer operating in the quantum Hall regime. *Proc. Natl. Acad. Sci. USA* **107**, 5276
7. Steinberg, H. Barak, G., Yacoby, A., Pfeiffer, L. N., West, K. W., Halperin, B. I. & Le Hur, K. Charge fractionalization in quantum wires. *Nature Phys.* **4**, 116-119 (2008).
8. Halperin, B. I. Quantized Hall conductance, current-carrying edge states, and the existence of extended states in a two-dimensional disordered potential. *Phys. Rev. B* **25**, 2185–2190 (1982).
9. Buttiker, M. Absence of backscattering in the quantum Hall effect in multi-probe conductors. *Phys. Rev. B* **38**, 9375–9389 (1988).
10. Kane, C. L., Fisher, M. P. A. & Polchinski, J. Randomness at the edge: theory of quantum Hall transport at filling $v=2/3$. *Phys. Rev. Lett.* **72**, 4129-4132 (1994).
11. Kane, C. L. & Fisher, M. P. A. Impurity scattering and transport of fractional quantum Hall edge states. *Phys. Rev. B* **51**, 13449-13466 (1995).
12. Bid, A., Ofek, N., Inoue, H., Heiblum, M., Kane, C. L., Umansky, V. & Mahalu, D. Observation of neutral modes in the quantum Hall regime. *Nature* **466**, 585-590 (2010).
13. Neder, I., Heiblum, M., Levinson, Y., Mahalu, D. & Umansky, V. Unexpected Behavior in a Two-Path Electron Interferometer. *Phys. Rev. Lett.* **96**, 016804 (2006).

14. Roulleau, P., Portier, Glattli, D. C., F., Roche, P., Cavanna, A., Faini, G., Gennser, U. & Mailly, D. Finite bias visibility of the electronic Mach-Zehnder interferometer. *Phys. Rev. B* **76**, 161309(R) (2007).
15. Neder, I., Heiblum, M., Mahalu, D. & Umansky, V. Controlled dephasing of electrons by non-gaussian shot noise. *Nat. Phys.* **3**, 534-537 (2007).
16. Roulleau, P., Portier, F., Roche, P., Cavanna, A., Faini, G., Gennser, U. & Mailly, D. Noise Dephasing in Edge States of the Integer Quantum Hall Regime. *Phys. Rev. Lett.* **101**, 186803 (2008).
17. Chalker, J. T., Gefen, Y. & Veillette, M. Y. Decoherence and interactions in an electronic Mach-Zehnder interferometer. *Phys. Rev. B* **76**, 085320 (2007).
18. Levkivskyi, I. P. & Sukhorukov, E. V. Dephasing in the electronic Mach-Zehnder interferometer at filling factor 2. *Phys. Rev. B* **78**, 045322 (2008).
19. Altimiras, C., Le Sueur, H., Gennser, U., Cavanna, A., Mailly, D. & Pierre, F. Non-equilibrium edge-channel spectroscopy in the integer quantum Hall regime. *Nat. Phys.* **6**, 34-39 (2010).
20. Le Sueur, H., Altimiras, C., Gennser, U., Cavanna, A., Mailly, D. & Pierre, F. Energy Relaxation in the Integer Quantum Hall Regime. *Phys. Rev. Lett.* **105**, 056803 (2010).
21. Lunde, A. M., Nigg, S. E. & Buttiker, M. Interaction-induced edge channel equilibration. *Phys. Rev. B* **81**, 041311(R) (2010).
22. Degiovanni, P., Greiter, C., Feve, G., Altimiras, C., Le Sueur, H. & Pierre, F. Plasmon scattering approach to energy exchange and high-frequency noise in $v=2$ quantum Hall edge channels. *Phys. Rev. B* **81**, 121302(R) (2010).
23. Kovrizhin, D. L. & Chalker, J. T. Equilibration of integer quantum Hall edge states. *Phys. Rev. B* **84**, 085105 (2011).
24. Berg, E., Oreg, Y. Kim, E. A. & von Oppen, F. Fractional Charges on an Integer Quantum Hall Edge. *Phys. Rev. Lett.* **102**, 236402 (2009).
25. Leinaas, J. M., Horsdal, M. & Hansson, T. H. Sharp fractional charges in Luttinger liquids. *Phys. Rev. B* **80**, 115327 (2009).
26. Horsdal, M., Rypestøl, M., Hansson, H. & Leinaas, J. M. Charge fractionalization on quantum Hall edges. *Phys. Rev. B* **84**, 115313 (2011).

27. Neder, I. Fractionalization noise in edge channels of integer quantum Hall effect. *Phys. Rev. Lett.* **108**, 186404 (2012).
28. Levkivskyi, I. P. & Sukhorukov, E. V. Shot-noise thermometry of the quantum Hall edge states. *Phys. Rev. Lett.* **109**, 246806 (2012).
29. Milletari, M. & Rosenow, B. Shot noise signature of charge fractionalization in the $v = 2$ quantum Hall edge, arXiv:1207.1719 (2012).
30. Bocquillon, E. *et al.* Separation of neutral and charge modes in one dimensional chiral edge channels. *Nat. Comm.* **4**, 1839 (2013).
31. Martin, T. & Landauer, R. Wave-packet approach to noise in multichannel mesoscopic systems. *Phys. Rev. B* **45**, 1742–1755 (1992).
32. Heiblum, M. Quantum shot noise in edge channels. *Phys. Status Solidi b* **243**, 3604–3616 (2006).
33. Chamon, de C. C., Freed, D. E. & Wen, X. G. Non-equilibrium quantum noise in chiral Luttinger liquids. *Phys. Rev. B* **53**, 4033–4053 (1996).

Figure 1

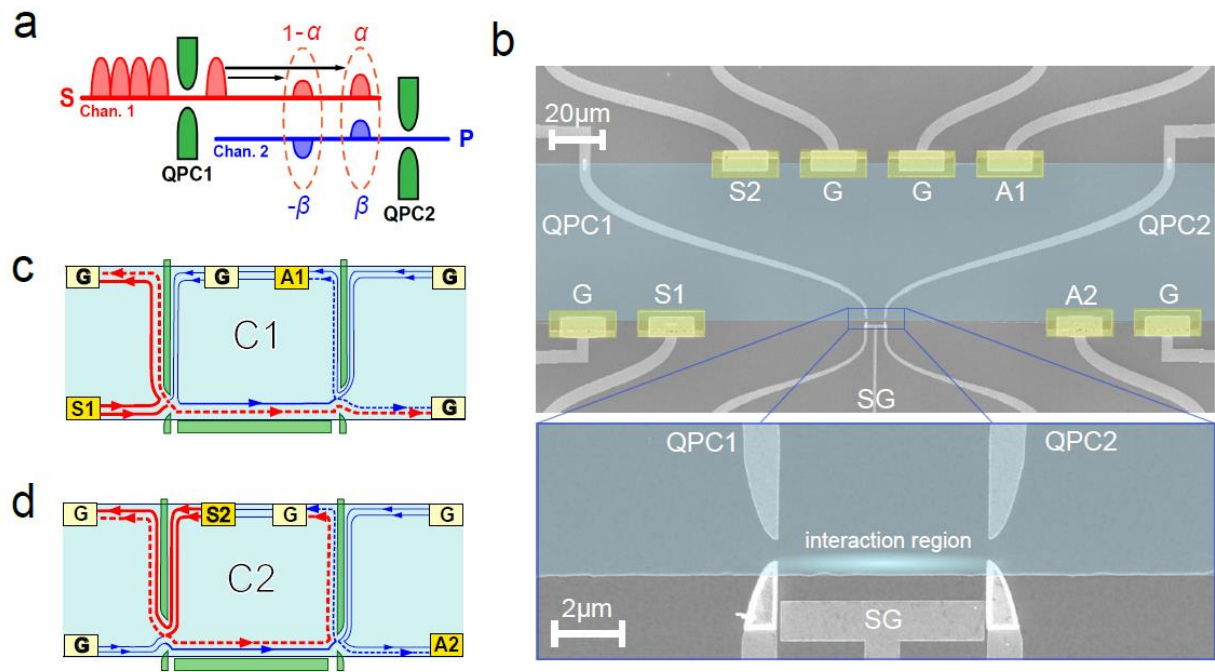


Figure 2

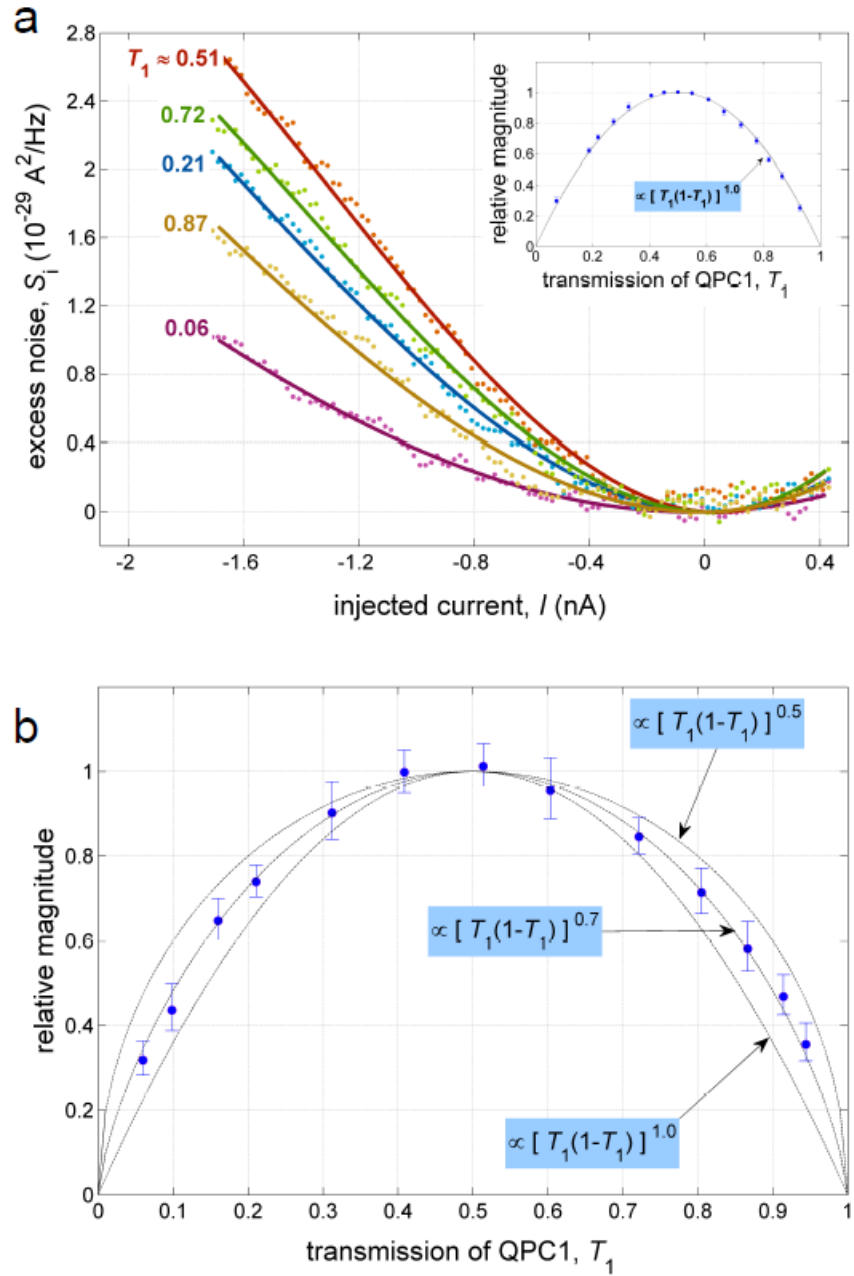


Figure 3

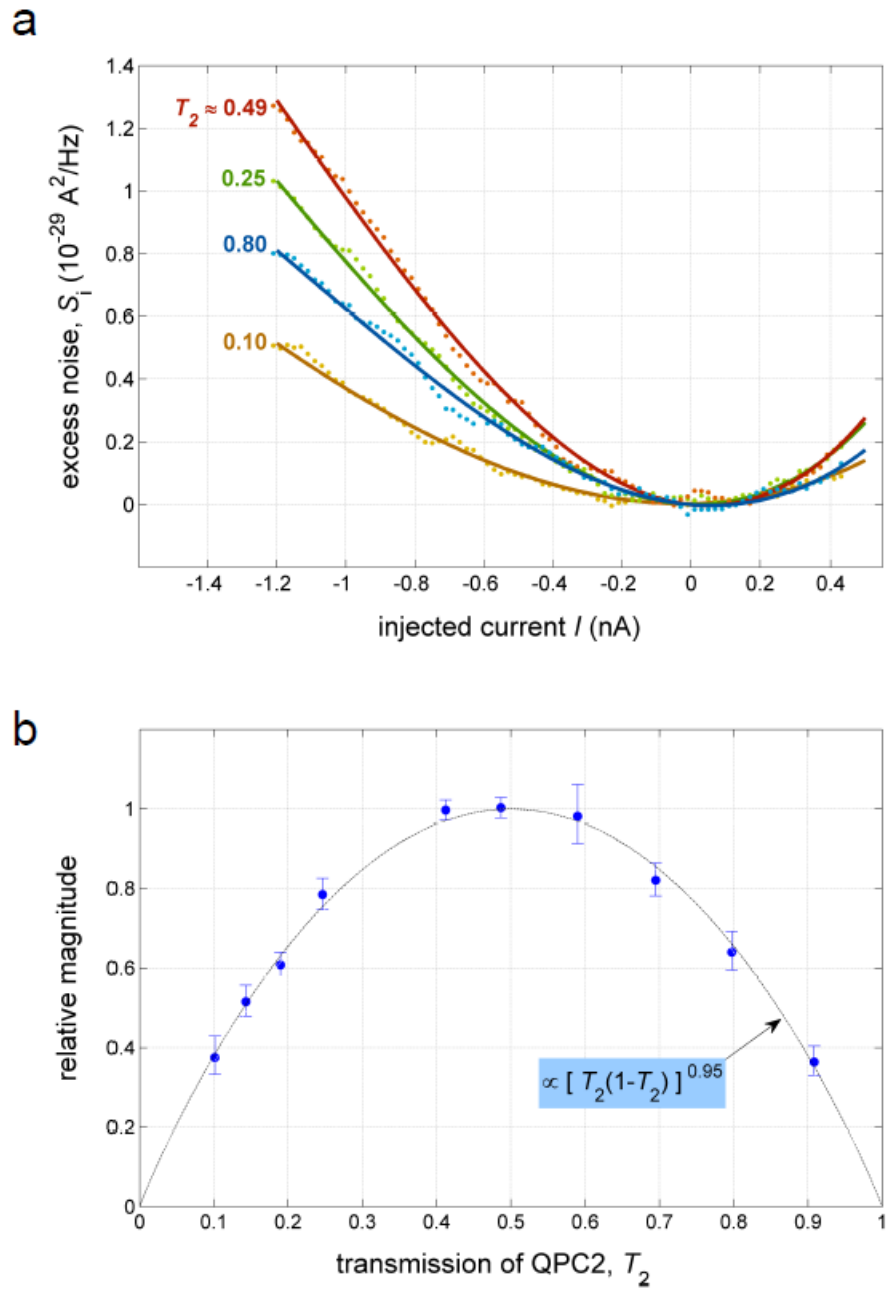


Figure4

